Stem Cell Research 77 (2024) 103410

Contents lists available at ScienceDirect

Stem Cell Research

journal homepage: www.elsevier.com/locate/scr

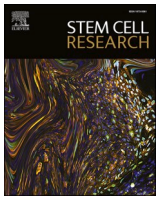

Lab Resource: Multiple Cell Lines

Generation of two iPSC lines from patients with inherited central core disease and concurrent malignant hyperthermia caused by dominant missense variants in the *RYR1* gene

Joshua S. Clayton [a,b,*], Christina Vo [a,b], Jordan Crane [a,b], Carolin K. Scriba [a,b,c], Safaa Saker [d], Thierry Larmonier [d], Edoardo Malfatti [e,f], Norma B. Romero [g,h], Gianina Ravenscroft [a,b], Nigel G. Laing [a,b], Rhonda L. Taylor [a,b]

[a] *Harry Perkins Institute of Medical Research, QEII Medical Centre, Nedlands, WA, Australia*
[b] *Centre for Medical Research, University of Western Australia, QEII Medical Centre, Nedlands, WA, Australia*
[c] *Neurogenetics Laboratory, Department of Diagnostic Genomics, PP Block, QEII Medical Centre, Nedlands, WA, Australia*
[d] *Genethon, DNA and Cell Bank, 91000 Evry, France*
[e] *APHP, Centre de Référence de Pathologie Neuromusculaire Nord-Est-Ile-de-France, Henri Mondor Hospital, France*
[f] *Université Paris Est, U955, INSERM, IMRB, F-94010 Créteil, France*
[g] *Sorbonne Université, Myology Institute, Neuromuscular Morphology Unit, Center for Research in Myology, GH Pitié-Salpêtrière, Paris, France*
[h] *Centre de Référence de Pathologie Neuromusculaire Paris-Est, GHU Pitié-Salpêtrière, Assistance Publique-Hôpitaux de Paris, Paris, France*

A B S T R A C T

RYR1 variants are the most common genetic cause of congenital myopathies, and typically cause central core disease (CCD) and/or malignant hyperthermia (MH). Here, we generated iPSC lines from two patients with CCD and MH caused by dominant *RYR1* variants within the central region of the protein (p.Val2168Met and p.Arg2508Cys). Both lines displayed typical iPSC morphology, uniform expression of pluripotency markers, trilineage differentiation potential, and had normal karyotypes. These are the first *RYR1* iPSC lines from patients with both CCD and MH. As these are common CCD/MH variants, these lines should be useful to study these conditions and test therapeutics.

Resource Table:

Unique stem cell lines identifier	1. HPIi006-A 2. HPIi007-A
Alternative name(s) of stem cell lines	1. RYR1-3278-R2A (HPIi006-A) 2. RYR1-6546-R3B (HPIi007-A)
Institution	Harry Perkins Institute of Medical Research
Contact information of distributor	Dr. Joshua Clayton joshua.clayton@perkins.org.au
Type of cell lines	iPSC
Origin	Human
Additional origin info required *for human ESC or iPSC*	1. HPIi006-A: 3 years, male, European (French) 2. HPIi007-A: 40 years, male, unknown ethnicity
Cell Source	Lymphoblastoid cell line (LCL) immortalized with Epstein Barr Virus
Clonality	Clonal
Method of reprogramming	Sendai virus (CytoTune-iPS 2.0^{TM})

(*continued on next column*)

(*continued*)

Unique stem cell lines identifier	1. HPIi006-A 2. HPIi007-A
Genetic Modification	Yes
Type of Genetic Modification	1. Inherited variant (dominant, inherited from affected father) 2. Inherited variant (dominant, 17 other affected family members across 6 generations)
Evidence of the reprogramming transgene loss (including genomic copy if applicable)	RT-PCR to confirm clearance of Sendai virus
Associated disease	Central core disease of muscle; CCD (OMIM# 117000), and Malignant hyperthermia susceptibility 1; MHS1 (OMIM# 180901)
Gene/locus	1. HPIi006-A: Ryanodine Receptor 1, Skeletal Muscle (*RYR1*), NM_000540.3: c.7522C > T (p.Arg2508Cys) 2. HPIi007-A: Ryanodine Receptor 1,

(*continued on next page*)

* Corresponding author at: Harry Perkins Institute of Medical Research, QEII Medical Centre, Nedlands, WA, Australia.
E-mail address: joshua.clayton@perkins.org.au (J.S. Clayton).

https://doi.org/10.1016/j.scr.2024.103410
Received 26 March 2024; Accepted 30 March 2024
Available online 30 March 2024

(*continued*)

Unique stem cell lines identifier	1. HPIi006-A 2. HPIi007-A
	Skeletal Muscle (*RYR1*), NM_000540.3: c.6502G > A (p.Val2168Met)
Date archived/stock date	Cell line stocks archived at Harry Perkins Institute, November 2022 (HPIi006-A) or December 2022 (HPIi007-A)
Cell line repository/bank	1. https://hpscreg.eu/cell-line/HPIi006-A 2. https://hpscreg.eu/cell-line/HPIi007-A
Ethical approval	Personnes (Est IV DC-2012-1693), and national consent forms for genetic testing, banking and research were signed by the patients or their legal guardian. The patient's LCLs were banked by Genethon; activity authorization No. AC-2018-3156, import/export authorization No. IE-2018-994. The study was approved by the University of Western Australia's Human Research Ethics Committee (approval number: RA/4/20/1008).

1. Resource utility

These are the first human iPSC lines derived from individuals with both central core disease (CCD) and malignant hyperthermia (MH) caused by *RYR1* variants. Both are common CCD/MH variants within the central RyR1 protein domain. Therefore, these lines are potentially useful tools to study CCD/MH in a human context.

2. Resource details

CCD is a highly heterogeneous myopathy characterized histologically by the presence of centrally located core-like areas in skeletal muscle fibres that are depleted of mitochondria (Jungbluth et al., 2011). CCD is slowly progressive and usually presents in childhood with muscle weakness and motor developmental delay (Jungbluth, 2007). Dominant variants in the *RYR1* gene are responsible for 50–90 % of cases (Fusto et al., 2022; Wu et al., 2006). A significant proportion of patients with CCD caused by *RYR1* variant/s also have MH – a pharmacogenetic disorder characterized by muscle rigidity which can cause a fatal increase in body temperature (Denborough et al., 1962; Rosenberg et al., 2007). Most *RYR1* variants associated with CCD and MH are dominant missense changes located in critical regions of the protein (Jungbluth et al., 2011).

Here, we generated and characterized iPSC lines from two unrelated patients with familial CCD and MH (Table 1). Both cases were caused by dominant missense changes within the bridging solenoid (Bsol) protein domain in the central region of RyR1 (residues 2,145–3,613) (Meissner, 2017). Both are common CCD/MH variants (Ibarra et al., 2006; Murayama et al., 2016; Wu et al., 2006). Patient 1 (HPIi006-A, p.Arg2508Cys) was diagnosed at age 3. They had slight motor delay, thin muscle bulk, scoliosis, and an elongated face with high-arched palate. At 15 years they suffered from multiple contractures. Patient 2 (HPIi007-A, p.Val2168Met) showed disease onset at 40 years with muscle weakness and difficulty walking.

Patient iPSCs were generated from lymphoblastoid cell lines (LCLs) using the CytoTune^{TM}-iPS 2.0 Sendai reprogramming kit. At passage 10 both lines showed typical iPSC morphology and no spontaneous differentiation (Fig. 1A), with uniform staining of pluripotency markers OCT4, SOX2, SSEA4, and TRA-1–60 by immunofluorescence (IF) (Fig. 1C, Fig. S1A). Likewise, transcript abundance of four pluripotency factors (*OCT4*, *SOX2*, *NANOG*, *CRIPTO*) was comparable or higher than a well-characterized control iPSC line, SCTi003-A (Fig. 1B). RT-PCR confirmed iPSCs were cleared of Sendai virus (Fig. 1D). No significant copy number abnormalities were identified by hPSC genetic analysis (Fig. S1B).

Both lines showed good mesoderm and ectoderm potential following directed differentiation (Fig. 1E). *TBX6* (mesoderm), *OTX2* and *PAX6* (ectoderm) expression was lower than for SCTi003-A (Fig. 1E), but IF revealed differentiations were equally homogenous between lines (Fig. S1C). HPIi007-A demonstrated good endoderm potential (comparable to control), although HPIi006-A showed much lower expression of endoderm markers (*GATA4* and *SOX17*) by qRT-PCR (Fig. 1E). IF confirmed that HPIi006-A endoderm cultures only contained a few areas of SOX17-positive cells, in contrast to highly homogenous populations in HPIi007-A and SCTi003-A (Fig. S1C). Although this might limit the potential of HPIi006-A in some ways, given the biological role and expression of RyR1 it is likely that cells would be exclusively differentiated to mesoderm and/or neuroectoderm for disease modelling purposes. Therefore, both lines should be equally suited for modelling

Table 1
Characterization and validation.

Classification	Test	Result	Data
Morphology	Photography Bright field	At P11: Normal morphology	Fig. 1 panel A
Phenotype	Qualitative analysis (immunocytochemistry)	At P11: Positive for OCT4, SOX2, SSEA4, TRA-1–60	Fig. 1 panel C, Supplementary Fig. 1 panel A
	Quantitative analysis (qRT-PCR)	At P10: Expression of *OCT4*, *SOX2*, *NANOG*, *CRIPTO*	Fig. 1 panel B
Genotype	Karyotype (G-banding) and resolution	At P13 (HPIi006-A), or P19 (HPIi007-A): 46, XY (normal male karyotype) Banding Resolution: 400 bands per haploid set 15 metaphases counted, 5 analyzed for each	Fig. 1 panel F; hPSC genetic analysis (P10): Supplementary Fig. 1 panel B
Identity	STR analysis	At P10: Matched to parental LCLs at 22/22 STR loci (note: HPIi006-A parental LCLs had spurious additional peak)	Available with authors
Mutation analysis	Sequencing	At P10: Heterozygous for *RYR1* c.7522C > T variant (HPIi006-A), or *RYR1* c.6502G > A variant (HPIi007-A)	Fig. 1 panel G
Microbiology and virology	Mycoplasma	At P13: Negative for mycoplasma by PCR	Mycoplasma: Supplementary Fig. 1 panel D
	Sendai virus (SeV)	At P10: Negative for SeV by RT-PCR	SeV: Fig. 1 panel D
	Epstein Barr virus (EBV)	At P10 (HPIi006-A) or P13 (HPIi007-A): Negative for EBV by PCR	EBV: Supplementary Fig. 1 panel E
Differentiation potential	Directed differentiation	At P14 (HPIi006-A) or P20 (HPIi007-A): Enrichment of *TBXT* and *TBX6* (mesoderm), *OTX2* and *PAX6* (ectoderm), and *SOX17* and *GATA4* (endoderm) by qRT-PCR. Enrichment of Brachyury (mesoderm), OTX2 (ectoderm) and SOX17 (endoderm) by immunocytochemistry	Fig. 1 panel E (qRT-PCR); Supplementary Fig. 1 panel C (immunofluorescence)
Donor screening (OPTIONAL)	HIV 1 + 2 Hepatitis B, Hepatitis C	Not performed	
Genotype additional info (OPTIONAL)	Blood group genotyping	Not performed	
	HLA tissue typing	Not performed	

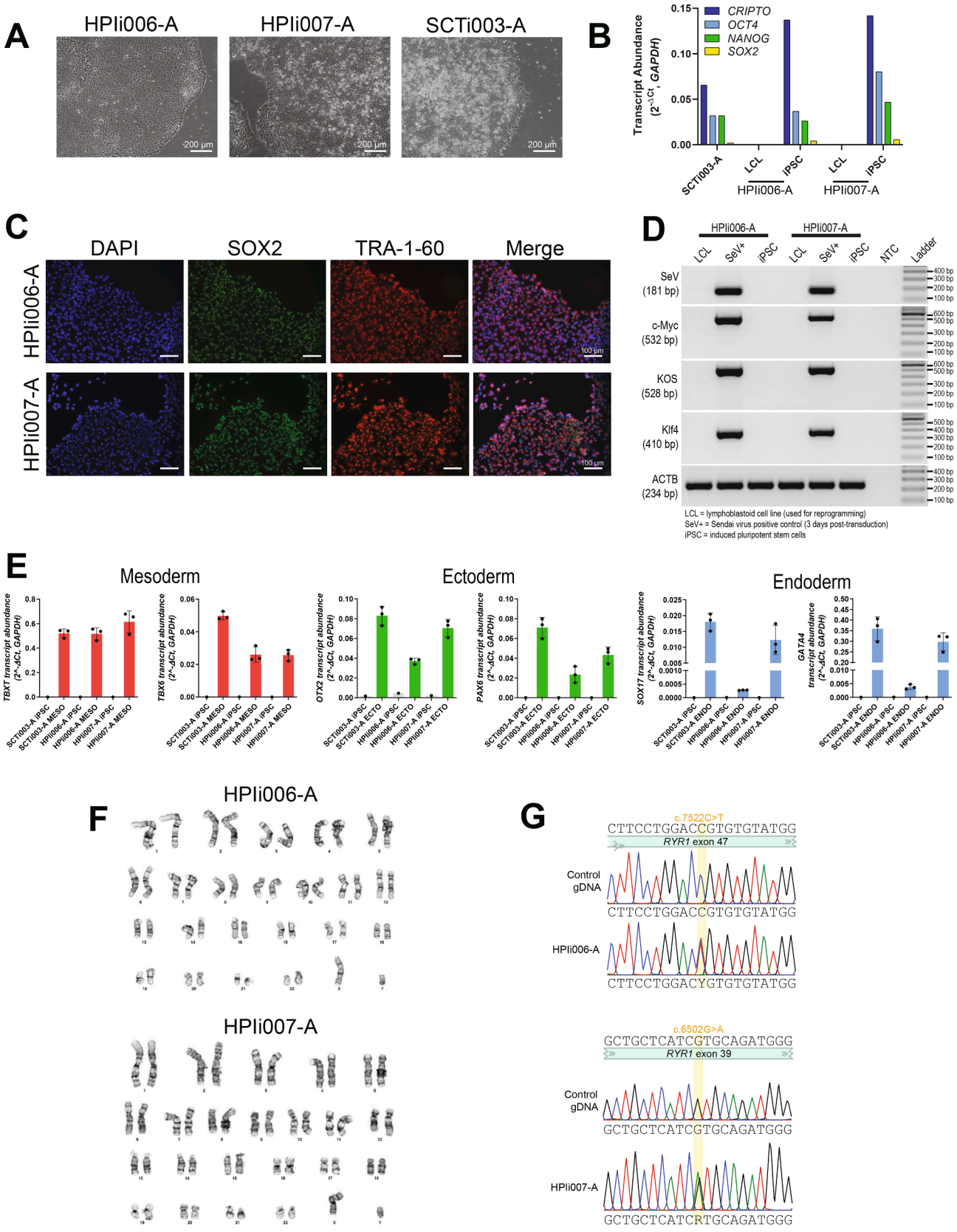

Fig. 1. Characterization of HPIi006-A and HPIi007-A iPSC lines.

neuromuscular disease pathology.

Both lines had a normal 46,XY male karyotype by G-banding (Fig. 1F), and STR profiles matched the original donors at all 22 tested loci (available with authors). The *RYR1* variants were both confirmed heterozygous by PCR and Sanger sequencing (Fig. 1G). Lines were also proven to be free of mycoplasma (Fig. S1D) and Epstein-Barr virus (Fig. S1E) by PCR.

3. Materials and methods

3.1. Reprogramming and maintenance of iPSC lines

Patient LCLs were cultured in RPMI-1640 medium supplemented with 10 % fetal bovine serum, 1 % L-glutamine, and 1 % penicillin–streptomycin (R10 medium). Reprogramming was performed

Table 2
Reagents details.

	Antibodies used for immunocytochemistry/flow-cytometry			
	Antibody	**Dilution**	**Company Cat #**	**RRID**
Pluripotency marker	Rabbit anti-OCT4	1:200	Thermo Fisher Cat# A24867	AB_2650999
Pluripotency marker	Mouse anti-SSEA4	1:100	Thermo Fisher Cat# A24866	AB_2651001
Pluripotency marker	Rat anti-SOX2	1:100	Thermo Fisher Cat# A24759	AB_2651000
Pluripotency marker	Mouse anti-TRA-1–60	1:100	Thermo Fisher Cat# A24868	AB_2651002
Secondary antibody	Alexa Fluor™ 594 donkey anti-rabbit	1:250	Thermo Fisher Cat# A21207	AB_141637
Secondary antibody	Alexa Fluor™ 488 goat anti-mouse IgG3	1:250	Thermo Fisher Cat# A24877	AB_2651008
Secondary antibody	Alexa Fluor™ 488 donkey anti-rat	1:250	Thermo Fisher Cat# A24876	AB_2651007
Secondary antibody	Alexa Fluor™ 594 goat anti-mouse IgM	1:250	Thermo Fisher Cat# A21044	AB_2535713
Differentiation marker (ectoderm)	Anti-human Otx-2 NL557-conjugated goat IgG	1:10	R&D systems Cat# SC022, Part# 967389	AB_2889887
Differentiation marker (mesoderm)	Anti-human Brachyury NL557-conjugated goat IgG	1:10	R&D systems Cat# SC022, Part# 967388	AB_2889887
Differentiation marker (endoderm)	Anti-human SOX17 NL637-conjugated goat IgG	1:10	R&D systems Cat# SC022, Part# 967393	AB_2889887

	Primers		
	Target	**Size of band**	**Forward/Reverse primer (5′-3′)**
Pluripotency markers (qPCR)	*OCT4*	63 bp	F: GGGTTTTTGGGATTAAGTTCTTCA/R: GCCCCCACCCTTTGTGTT
	SOX2	63 bp	F: CAAAAATGGCCATGCAGGTT/R: AGTTGGGATCGAACAAAAGCTATT
	NANOG	111 bp	F: ACAACTGGCCGAAGAATAGCA/R: GGTTCCCAGTCGGGTTCAC
	CRIPTO	66 bp	F: CGGAACTGTGAGCACGATGT/R: GGGCAGCCAGGTGTCATG
Mesoderm markers (qPCR)	*TBXT*	109 bp	F: GGTCCAGCCTTGGAATGCCT/R: CCGTTGCTCACAGACCACAG
	BMP4	135 bp	F: GCACTGGTCTTGAGTATCCTG/R: TGCTGAGGTTAAAGAGGAAACG
Endoderm markers (qPCR)	*SOX17*	102 bp	F: GTGGACCGCACGGAATTTGA/R: GCTGTCGGGGAGATTCACAC
	GATA4	100 bp	F: CAGCGAGGAGATGCGTCC/R: AGACATCGCACTGACTGAGAA
Ectoderm markers (qPCR)	*OTX2*	106 bp	F: GACCCGGTACCCAGACATCTT/R: GCGGCACTTAGCTCTTCGATT
	PAX6	120 bp	F: AACGATAACATACCAAGCGTGT/R: GGTCTGCCCGTTCAACATC
House-keeping Genes (qPCR)	*GAPDH*	148 bp	F: TCGGAGTCAACGGATTTGGT/R: TTGCCATGGGTGGAATCATA
Sendai virus vectors (RT-PCR)	Sendai virus (SeV) genome	181 bp	F: GGATCACTAGGTGATATCGAGC/R: ACCAGACAAGAGTTTAAGAGATATGTATC
	KOS transgene	528 bp	F: ATGCACCGCTACGACGTGAGCGC/R: ACCTTGACAATCCTGATGTGG
	Klf4 transgene	410 bp	F: TTCCTGCATGCCAGAGGAGCCC/R: AATGTATCGAAGGTGCTCAA
	c-Myc transgene	532 bp	F: TAACTGACTAGCAGGCTTGTCG/R: TCCACATACAGTCCTGGATGATGATG
House-keeping genes (RT-PCR)	*ACTB*	234 bp	F: GGACTTCGAGCAAGAGATGG/R: AGCACTGTGTTGGCGTACAG
EBV testing (PCR)	*BZLF-1*	637 bp	F: CACCTCAACCTGGAGACAAT/R: TGAAGCAGGCGTGGTTTCAA
	LMP1	617 bp	F: ATGGAACACGACCTTGAGA/R: TGAGCAGGATGAGGTCTAGG
	OriP	544 bp	F: TCGGGGGTGTTAGAGACAAC/R: TTCCACGAGGGTAGTGAACC
House-keeping Genes (PCR)	*GAPDH*	452 bp	F: ACCACAGTCCATGCCATCAC/R: TCCACCACCCTGTTGCTGTA
Targeted mutation analysis (PCR/sequencing) – HPIi006-A	*RYR1* (R primer used for Sanger sequencing)	468 bp	F: CCAGCTAATCCAAGCCGGCAAG R: TGCTGCTGCTCTACCGTGAC
Targeted mutation analysis (PCR/sequencing) – HPIi007-A	*RYR1* (F primer used for Sanger sequencing)	376 bp	F: TGCATGGTGCTCCAAGCCTTG R: GTATCCTGAGGGTATTCATTACCCAAGG

with the CytoTune™-iPS 2.0 Sendai Reprogramming Kit (ThermoFisher) using 3×10^5 cells. Cells were plated on growth factor-reduced (GFR) Matrigel® (Corning; diluted 1:100 in DMEM/F12) and gradually transitioned from R10 to ReproTeSR™ (StemCell Technologies). Individual clones were picked and expanded in mTeSR™ Plus (StemCell Technologies) on GFR Matrigel. Following three rounds of manual picking, cells were routinely passaged with 1X Versene (ThermoFisher) at 1:12–1:20 with 10 μM ROCK inhibitor (Y-27632). Cells were cryopreserved in 90 % KnockOut™ Serum Replacement (ThermoFisher) with 10 % DMSO (Sigma). The control iPSC line SCTi003-A was purchased from StemCell Technologies and maintained as above. All cells were maintained at 37 °C and 5 % CO_2.

3.2. Trilineage differentiation

Directed differentiation was performed using the STEMdiff™ trilineage differentiation kit (StemCell Technologies). Cell pellets were collected using 1X TrypLE Express (Gibco).

3.3. Immunocytochemistry

Cells were fixed in 4 % paraformaldehyde for 15 min at room temperature (RT) and washed three times in 1X DPBS. Pluripotency staining was performed using the PSC 4-marker Immunocytochemistry Kit (Thermo Fisher). Germ layer staining was carried out per the Human Three Germ Layer 3-Color Immunocytochemistry Kit (SC022, R&D Systems). All primary antibody staining was performed overnight at 4 °C. Nuclei were stained with NucBlue™ Fixed Cell Stain for 10 min at RT (ThermoFisher). Samples were imaged on an Olympus IX71 with DP74 camera and CellSens software, or a CellInsight CX7 (SOX17 only due to NL637 conjugation).

3.4. DNA and RNA extraction

Genomic DNA was extracted using the QIAamp DNA Mini Kit (Qiagen). RNA was extracted using the RNeasy Mini Kit (Qiagen) and cDNA synthesized using the SuperScript™ III First-Strand Synthesis System (ThermoFisher).

3.5. Polymerase chain reaction (PCR)

Standard PCRs were performed using GoTaq® G2 Hot Start Mastermix (Promega) and a C1000 thermocycler (Bio-Rad). Cycling conditions for EBV and SeV detection: 95 °C/2 min, (95 °C/30 s, 60 °C/30 s and 72 °C/40 s) × 35, 72 °C/5 min; *RYR1* variant confirmation: 95 °C/5 min, (95 °C/30 s, 65 °C/30 s −0.5 °C/cycle, 72 °C/30 s) × 15, (98 °C/30 s, 57 °C/30 s, 72 °C/30 s) × 30, 72 °C/5 min. Primers are listed in Table 2.

3.6. Quantitative PCR (qRT-PCR)

qRT-PCRs were performed using the Rotor-Gene SYBR Green RT-PCR Kit (Qiagen) on a Rotor-Gene Q thermocycler using the following cycling conditions: 95 °C/5 min, (95 °C/10 s, 60 °C/15 s) × 45 cycles, followed by melt curve analysis. Data were normalized to *GAPDH* using the ΔC_T method. Primers are listed in Table 2.

3.7. Sanger sequencing

PCR products were purified using the MinElute PCR Purification Kit (Qiagen). Sanger sequencing was done by the Australian Genome Research Facility (Perth, WA, Australia).

3.8. Mycoplasma testing

All lines were screened for mycoplasma using the ATCC Universal Mycoplasma Contamination Kit.

3.9. Karyotyping

iPSCs were screened for common karyotypic abnormalities using the hPSC Genetic Analysis Kit (StemCell Technologies) on a Bio-Rad CFX. G-banding was performed by PathWest Diagnostic Genomics (Perth, WA, Australia).

3.10. Short tandem repeat (STR) typing

STR typing was performed at PathWest Diagnostic Genomics (Perth, WA, Australia) using the QSTR Plus assay (Elucigene).

3.11. Graphs and statistics

Graphs and statistics were done using GraphPad Prism 9.1.2.

CRediT authorship contribution statement

Joshua S. Clayton: Conceptualization, Data curation, Formal analysis, Funding acquisition, Investigation, Methodology, Project administration, Supervision, Writing – original draft. **Christina Vo:** Data curation, Formal analysis. **Jordan Crane:** Data curation, Formal analysis. **Carolin K. Scriba:** Data curation, Formal analysis. **Safaa Saker:** Resources. **Thierry Larmonier:** Resources. **Edoardo Malfatti:** Data curation, Formal analysis, Investigation, Resources. **Norma B. Romero:** Data curation, Formal analysis, Project administration, Resources. **Gianina Ravenscroft:** Writing – review & editing, Funding acquisition, Supervision. **Nigel G. Laing:** Funding acquisition, Supervision, Writing – review & editing. **Rhonda L. Taylor:** Conceptualization, Data curation, Formal analysis, Funding acquisition, Project administration, Supervision, Writing – review & editing.

Declaration of competing interest

The authors declare the following financial interests/personal relationships which may be considered as potential competing interests: Rhonda Taylor reports financial support was provided by Stan Perron Charitable Foundation.

Data availability

Data will be made available on request.

Acknowledgements

This work was supported by funding from the Stan Perron Charitable Foundation (202003010Research), awarded to Rhonda Taylor. We also gratefully acknowledge funding from the Australian National Health and Medical Research Council (NHMRC), including an EL2 Investigator Grant (APP2007769) to Gianina Ravenscroft. Rhonda Taylor is supported by a Raine Priming Grant (RPG54-21) from the Raine Medical Research Foundation. We also wish to gratefully acknowledge Dr Susan Treves for her intellectual input.

Appendix A. Supplementary data

Supplementary data to this article can be found online at https://doi.org/10.1016/j.scr.2024.103410.

References

Denborough, M.A., Forster, J.F.A., Lovell, R.R.H., Maplestone, P.A., Villiers, J.D., 1962. Anaesthetic deaths in a family. Br. J. Anaesth. 34, 395–396. https://doi.org/10.1093/bja/34.6.395.

Fusto, A., Cassandrini, D., Fiorillo, C., Codemo, V., Astrea, G., D'Amico, A., Maggi, L., Magri, F., Pane, M., Tasca, G., Sabbatini, D., Bello, L., Battini, R., Bernasconi, P., Fattori, F., Bertini, E.S., Comi, G., Messina, S., Mongini, T., Moroni, I., Panicucci, C., Berardinelli, A., Donati, A., Nigro, V., Pini, A., Giannotta, M., Dosi, C., Ricci, E., Mercuri, E., Minervini, G., Tosatto, S., Santorelli, F., Bruno, C., Pegoraro, E., 2022. Expanding the clinical-pathological and genetic spectrum of RYR1-related congenital myopathies with cores and minicores: an Italian population study. Acta Neuropathol. Commun. 10, 1–20. https://doi.org/10.1186/s40478-022-01357-0.

Ibarra, M.C.A., Wu, S., Murayama, K., Minami, N., Ichihara, Y., Kikuchi, H., Noguchi, S., Hayashi, Y.K., Ochiai, R., Nishino, I., 2006. Malignant hyperthermia in Japan. Anesthesiology 104, 1146–1154. https://doi.org/10.1097/00000542-200606000-00008.

Jungbluth, H., 2007. Central core disease. Orphanet J. Rare Dis. 2, 25. https://doi.org/10.1186/1750-1172-2-25.

Jungbluth, H., Sewry, C.A., Muntoni, F., 2011. Core myopathies. Semin. Pediatr. Neurol. 18, 239–249. https://doi.org/10.1016/j.spen.2011.10.005.

Meissner, G., 2017. The structural basis of ryanodine receptor ion channel function. J. Gen. Physiol. 149, 1065–1089. https://doi.org/10.1085/jgp.201711878.

Murayama, T., Kurebayashi, N., Ogawa, H., Yamazawa, T., Oyamada, H., Suzuki, J., Kanemaru, K., Oguchi, K., Iino, M., Sakurai, T., 2016. Genotype-phenotype correlations of malignant hyperthermia and central Core disease mutations in the central region of the RYR1 channel. Hum. Mutat. 37, 1231–1241. https://doi.org/10.1002/humu.23072.

Rosenberg, H., Davis, M., James, D., Pollock, N., Stowell, K., 2007. Malignant hyperthermia. Orphanet J. Rare Dis. 2, 21. https://doi.org/10.1186/1750-1172-2-21.

Wu, S., Ibarra, M.C.A., Malicdan, M.C.V., Murayama, K., Ichihara, Y., Kikuchi, H., Nonaka, I., Noguchi, S., Hayashi, Y.K., Nishino, I., 2006. Central core disease is due to RYR1 mutations in more than 90% of patients. Brain 129, 1470–1480. https://doi.org/10.1093/brain/awl077.